Eur. Phys. J. D (2017) 71: 17
DOI: 10.1140/epjd/e2016-70596-3

THE EUROPEAN PHYSICAL JOURNAL D

Regular Article

Theoretical study of (e, 2e) process of atomic and molecular targets*

Salim Houamer[1,a], Mehdi Chinoune[1,2], and Claude Dal Cappello[3]

[1] LPQSD, Department of Physics, Faculty of Sciences, University Sétif 1, 19000 Sétif, Algeria
[2] USTHB, Faculty of Physics, Department of Theoretical Physics, 16111 Algiers, Algeria
[3] SRSMC, UMR CNRS 7565, University of Lorraine, BP 70239, 54506 Vandœuvre-les-Nancy, France

Received 26 September 2016 / Received in final form 15 November 2016
Published online 24 January 2017 –

Abstract. Triple differential ionization cross sections (TDCSs) by electron impact are calculated for some atomic and molecular targets by using several models where Post Collisional Interaction (PCI) is taken in account. We also investigate the effect of the short range potential and describe the ejected electron either by a Coulomb wave or by a distorted wave. Significant differences are observed between these models. A better agreement with experimental data is achieved when the short range potential and distortion effects are included.

1 Introduction

Ionization of matter by electron impact is a fundamental process in collision theory which plays a significant role in many fields such as plasma physics and astrophysics. One of the most important challenging tasks is the understanding of the collision details which still attracts interest nowadays [1–3]. The triply differential cross section (TDCS) obtained in (e, 2e) experiments where the two outgoing electrons are detected in coincidence represents the most detailed description of the ionization process. This quantity is evaluated through the scattering amplitude defined as the transition elements between the initial and the final states of the collision and is known to be a useful tool to probe the reaction dynamics [4,5] as well as the structure of the target [6,7]. There are hence been a long interest in obtaining TDCSs for electron impact ionization of atoms [8–10] and molecules [11–13] where many theoretical developments have allowed for accurate numerical calculations. The DWBA [14–17] is among the most successful theoretical approaches for rather complicated targets since it reproduces generally the dominant features of the TDCS for a projectile energy of about 100 eV and larger. This model takes into account the distorting effects of the target potential on the continuum electron states in the field of the residual ion. Subsequently the application of more sophisticated non perturbative methods like the CCC [18,19] or R-matrix models [20,21], based upon a powerful numerical scheme, provided results with excellent agreement with experiments.

When the two outgoing electrons are detected with comparable energies the post collision interaction (PCI) should be included. The PCI effects have been introduced in the final state via the work of Brauner et al. [22] (known as BBK). This BBK model gives a good agreement with experiments for light atoms but fails unfortunately for more complex atomic or molecular targets because the recoil peak is not generally well reproduced. The failure of BBK in reproducing the recoil peak is due to the fact that distortion effects are completely ignored. At low impact energy, second Born treatments where a double interaction between the projectile and the target is included, constitute also good frameworks to study the ionization process [23,24]. These models are at least rather appropriate to explain the lack of symmetry about the momentum transfer direction in the experimental data.

Nowadays the 3DW model applied for atoms [25,26] and extended successfully as M3DW to molecules [27,28] remain the most accurate description to calculate the TDCS. Within this non first order model, the PCI is contained to all orders of perturbation theory while all interactions contained in the perturbation operator are of first order. Owing to abundant available theoretical and experimental results in coincidence measurements where good agreement was achieved in many cases for atoms, the problem of (e, 2e) processes was considered to be well investigated. Unfortunately even with the most sophisticated models some discrepancies between theory and experiments have been observed for heavy atoms [29,30]. For molecules the disagreements observed are not surprising owing to the complexity of the molecular structure [31,32].

* Contribution to the Topical Issue "Many Particle Spectroscopy of Atoms, Molecules, Clusters and Surfaces", edited by A.N. Grum-Grzhimailo, E.V. Gryzlova, Yu V. Popov, and A.V. Solov'yov.

[a] e-mail: s_houamer@univ-setif.dz

In this paper we study the electron impact ionization of some atomic and molecular targets using non first order models. We use the BBK and BBKDW models which have been very recently investigated [33] where the interaction between the projectile and the target is purely Coulombic. We also apply the BBKSR model where further to the Coulombic interaction, the short range potential is included. Furthermore, the one active electron approximation is made to study (e, 2e) processes in the present work.

The paper is organized as follows. A summary of the theory is given in Section 2. Our results are discussed in Section 3 and compared with experiments. Finally, a conclusion is given in Section 4.

Atomic units are used throughout unless otherwise indicated.

2 Theory

The ionization of an atomic or molecular target by an electron may be schematized as:

$$e^- + A \rightarrow A^+ + e^- + e^-. \tag{1}$$

The TDCS corresponding to an (e, 2e) process is written as:

$$\sigma^{(3)} = \frac{d^3\sigma}{d\Omega_a d\Omega_b dE_b} = \frac{k_a k_b}{k_0} |T_{if}|^2 \tag{2}$$

where $d\Omega_a$ and $d\Omega_b$ denote respectively the elements of solid angles for the scattered and ejected electrons while dE_e is the variation of the ejection energy.

The conservation laws dealing with the ionization process are:

$$\frac{k_0^2}{2} = \frac{k_a^2}{2} + \frac{k_b^2}{2} - I$$

and

$$\vec{k}_0 = \vec{k}_a + \vec{k}_b + \vec{q}$$

where $\vec{k}_0$, $\vec{k}_a$, and $\vec{k}_b$ represent respectively the momenta of the incident, scattered, and ejected electrons. I and $\vec{q}$ are the energy needed to extract one electron from the target and the ion recoil momentum respectively. The matrix element T_{if} represents the transition from the initial state Ψ_i to the final state Ψ_f and is written as:

$$T_{if} = \langle \Psi_f | V | \Psi_i \rangle . \tag{3}$$

By using the one active electron approximation, the initial state is approximated by the initial bound state times a plane wave describing the incoming electron that is:

$$\Psi_i \left(\vec{k}_i, \vec{r}_0, \vec{r}_1\right) = \varphi_p \left(\vec{r}_0\right) \varphi_i \left(\vec{r}_1\right) \tag{4}$$

where $\varphi_p(\vec{k}_i, \vec{r}_0)$ is the plane wave describing the incident electron and $\varphi_i(\vec{r}_1)$ represents the one electron wave function of the target. $\vec{r}_0$ and $\vec{r}_1$ are the positions of the projectile and the bound electron with respect to the center of mass of the system.

All the individual atomic bound electrons are represented by linear combinations of Slater type wave functions [34]. The molecular orbitals are represented by linear combinations of single center wave functions of Moccia [35–37] which have been described enough in our previous papers [38,39].

The final state Ψ_f as well as the interaction potential V between the projectile and the target are written according to the corresponding model. The main feature of our theoretical approaches is that PCI effects are systematically included. Details about all used models are provided in the following.

2.1 The BBK model

Briefly, the BBK model [22] takes in account for the PCI which is included in the final state Ψ_f instead in the perturbation. The advantage of BBK is due to the fact that the PCI is contained to all orders of the perturbation theory. The final state Ψ_f is thus represented by two Coulomb waves describing the interaction of the outgoing electrons with the residual ion as well as a Coulomb interaction accounting for the PCI between the two electrons so that Ψ_f is written as:

$$\Psi_f \left(\vec{k}_a, \vec{k}_b, \vec{r}_0, \vec{r}_1\right) = \varphi_C \left(\vec{k}_a, \vec{r}_0\right) \varphi_C \left(\vec{k}_b, \vec{r}_1\right) \times C \left(\alpha_{01}, \vec{k}_{01}, \vec{r}_{01}\right). \tag{5}$$

The Coulomb wave $\varphi_C(\vec{k}, \vec{r})$ is given by:

$$\varphi_C \left(\vec{k}, \vec{r}\right) = \frac{\exp\left(i\vec{k}\cdot\vec{r}\right)}{(2\pi)^{3/2}} {}_1F_1 \left(-i\frac{Z}{k}, 1, -i\left(\vec{k}\cdot\vec{r} + kr\right)\right) \times \exp\left(\frac{\pi Z}{2k}\right) \Gamma\left(1 + i\frac{Z}{k}\right) \tag{6}$$

where the effective charge is generally taken to be $Z = 1$ in an (e, 2e) process.

$C(\alpha_{01}, \vec{k}_{01}, \vec{r}_{01})$ represents the PCI and is written as:

$$C \left(\alpha_{01}, \vec{k}_{01}, \vec{r}_{01}\right) = \exp\left(-\frac{\pi}{4\,k_{01}}\right) \Gamma\left(1 - \frac{i}{2k_{01}}\right) {}_1F_1 \times \left(-i\alpha_{01}, 1, -i\left(\vec{k}_{01}\cdot\vec{r}_{01} + k_{01}r_{01}\right)\right) \tag{7}$$

with

$$\vec{k}_{01} = \frac{1}{2}\left(\vec{k}_a - \vec{k}_b\right) \quad \text{and} \quad \alpha_{01} = -\frac{1}{2k_{01}}.$$

The calculation of the matrix element in equation (3) within the BBK model represents a real challenge due to the numerical difficulties associated with the evaluation of a six-dimensional integral. We apply here the method of Kornberg and Miraglia [40] where Fourier transforms are used to reduce the six-dimensional integral to a three-dimensional one.

In the BBK model the interaction between the projectile and the target V is purely Coulombic. By using the one active electron approximation, V is expressed as:

$$V\left(\vec{r}_0,\vec{r}_1\right)=\frac{1}{r_{01}}-\frac{1}{r_0} \tag{8}$$

where $r_{01}=|\vec{r}_0-\vec{r}_1|$ is the distance between the projectile and the bound electron.

2.2 The BBKDW model

The BBKDW model is a generalization of BBK where distorted effects are partially taken into account. The ejected electron is represented by a distorted wave instead of a Coulomb wave so that the final state is now written as:

$$\Psi_f\left(\vec{k}_a,\vec{k}_b,\vec{r}_0,\vec{r}_1\right)=\varphi_C\left(\vec{k}_a,\vec{r}_0\right)\,\varphi_{DW}\left(\vec{k}_b,\vec{r}_1\right)\times C\left(\alpha_{01},\vec{k}_{01},\vec{r}_{01}\right). \tag{9}$$

This model has been very recently used to investigate the ionization process of some atomic and molecular targets [33] where very good agreement was observed for the ionization of argon $(2p)$. Nevertheless the recoil region was not well reproduced especially in the case of the recent measurements of Isik et al. [41] for CH_4 molecule. The model is applied here to calculate the TDCS for atoms and molecules by considering other experimental kinematics.

We remind that in the distorted wave $\varphi_{DW}(\vec{k}_b,\vec{r})$ description the ejected electron sees a variable charge $Z(r)$ while leaving the target. The variable charge is such that $Z(r)=Z$ at $r=0$ and $Z(r)=1$ at $r_1\to\infty$. Z is the charge in the center of the residual ion.

Briefly, to calculate $Z(r)$ we use the spherically symmetric potential $U_j(r)$ representing the interaction between the projectile with the ionized targets. For atoms this potential is given by:

$$U_i(r)=\frac{1}{4\pi}\int V_j\left(\vec{r}\right)\,d\Omega=-\frac{Z\left(r\right)}{r} \tag{10a}$$

where

$$V_j\left(\vec{r}\right)=-\frac{Z}{r}+\sum_{i=1}^{N_0}N_{ij}\int\frac{\left|\varphi_i\left(\vec{r}\right)\right|^2}{|\vec{r}-\vec{r}_1|}d\vec{r}_1 \tag{10b}$$

where N_0 is the number of orbitals, N_{ij} is the number of electrons in the core orbital, Z the charge of the nuclei and $\varphi_i\left(\vec{r}\right)$ are the bound electron wave functions. A full description about the calculation of $Z(r)$in the case of atoms and molecules can be found in our previous works [33,42].

2.3 The BBKSR model

The BBKSR model is still an extension of the BBK model where the final state is represented by equation (5) like in BBK approach. Nevertheless the interaction between the projectile and the target is no longer purely Coulombic but includes in addition to this the short range potential.

To evaluate the short range potential in the one single active electron picture, the interaction between the projectile and the target is approximated as:

$$V_i=\frac{1}{r_{01}}+U_i \tag{11}$$

U_i is the spherically symmetric interaction potential between the projectile and the active electron and is obtained by averaging the anisotropic potential U_a so that:

$$U_i\left(r_0\right)=\frac{1}{4\pi}\int U_a\left(\vec{r}_0\right)\,d\Omega_0 \tag{12}$$

with:

$$U_a\left(\vec{r}_0\right)=-\frac{2}{r_0}+\int\frac{\left|\varphi_i\left(\vec{r}\right)\right|^2}{|\vec{r}_0-\vec{r}_1|}d\vec{r}_1. \tag{13}$$

After performing all calculations in equations (11) and (12), the spherically symmetric potential U_i takes finally the form:

$$U_i=-\frac{1}{r_0}+V_{SR}. \tag{14}$$

Comparing equations (11) and (14), the interaction potential between the projectile and the target writes:

$$V_i=\frac{1}{r_{01}}-\frac{1}{r_0}+V_{SR} \tag{15}$$

V_i may be interpreted as a pure Coulombic interaction plus a short range potential V_{SR} which tends asymptotically to zero. It should be mentioned that the short range potential is evaluated analytically for both atoms and molecules.

As an illustration, if we consider the helium atom in its ground state represented by the one-active electron orbital:

$$\varphi_{1s}\left(\vec{r}_1\right)=\varphi_{Hy}\left(\vec{r}_1\right)=\frac{\alpha^{3/2}}{\sqrt{\pi}}e^{-\alpha\,r_1}\quad\text{with}\quad\alpha=\frac{27}{16} \tag{16}$$

the short range potential V_{SR} is expressed as:

$$V_{SR}(r)=-\left(1+\alpha\,r\right)\,\frac{e^{-2\alpha\,r}}{r}.$$

We finally remind that the TDCS for molecules is obtained by averaging over Euler angles owing to the random orientation of molecular targets. The TDCS is defined as:

$$\sigma^{(3)}=\frac{1}{8\pi^2}\int\sigma^{(4)}d\Omega_{Euler} \tag{17}$$

where $\sigma^{(4)}$ is given by:

$$\sigma^{(4)}=\frac{d^4\sigma}{d\Omega_{Euler}d\Omega_a d\Omega_b dE_b}. \tag{18}$$

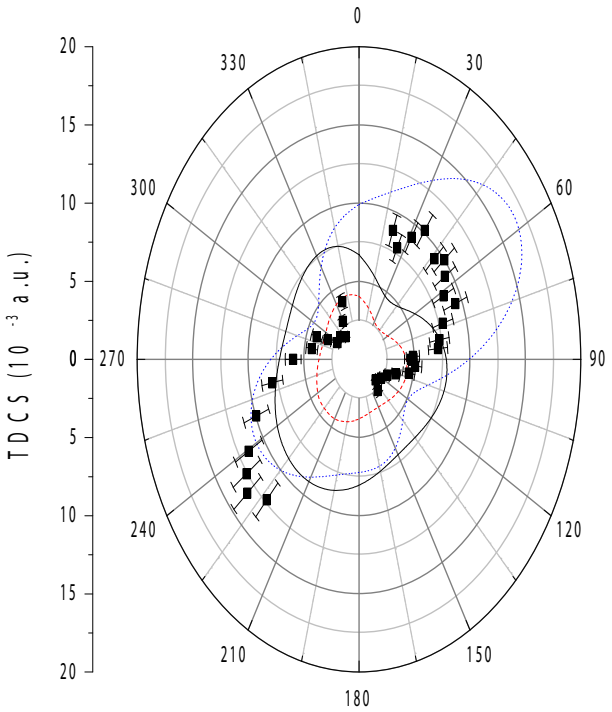

Fig. 1. Polar plot of the absolute TDCS for the $2p$ ionization of argon in 10^{-3} au. The scattered electron with an energy $E_a = 8000$ eV is detected at an angle $\theta_a = 1.25°$ in coincidence with the ejected electron with an energy $E_b = 150$ eV. Full squares are the absolute experimental data [44], with the one standard deviation statistical error bar. Comparison is made with the theoretical models: (i) the BBKSR model (black solid line); (ii) the BBK model (red dashed line); (iii) the BBKDW model (blue dotted line).

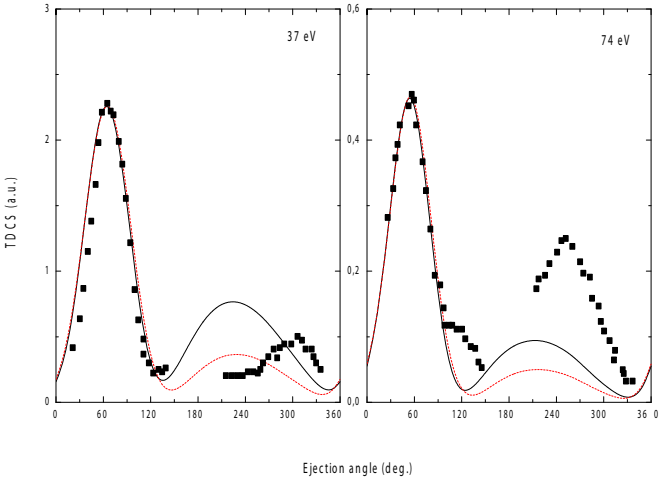

Fig. 2. Triple differential cross section for the $3p$ ionization of argon in its ground state. The scattered electron with an energy $E_a = 500$ eV is detected at an angle $\theta_a = 6°$ in coincidence with the ejected electron with energies $E_b = 37$ eV and $E_b = 74$ eV. Comparison is made between the experimental data (solid squares) taken from [45] and the theoretical models: (i) the BBKSR model (black solid line); (ii) the BBK model (red dashed line). The experiments are normalized to the absolute scale of BBKSR for the best visual fit at the maximum of the binary region.

3 Results and discussion

In this paper we present theoretical calculations based upon BBK, BBKDW and BBKSR models to investigate first the ionization of argon for which a large set of data is available. We consider thereafter some molecular targets which have been previously studied and where clear disagreements remain still observed even with sophisticated treatments [33,42,43]. The molecular targets CH_4, NH_3 and H_2O will be particularly investigated. We should indicate that BBKDW model faces large numerical problems, results based upon this model are thus presented only in few cases studied here.

The asymmetric coplanar TDCS for electron impact ionization of argon is presented in Figures 1 and 2 with a comparison between our theoretical models as well as experiments. In Figure 1, the TDCS of (e, 2e) on Ar ($2p$) orbital is presented for an impact energy of about 8 keV with a scattering angle of 1.25° and compared with absolute measurements [44]. These experiments exhibit two lobes, the recoil lobe is even larger than the binary one. The BBK and BBKSR models are in worse qualitative agreement with the data. On the contrary BBKDW shows a better agreement with experiments presenting as in the measured data the binary and recoil peaks. The binary region need still to be improved, the inclusion of the short range potential in BBKDW should likely provide a better description of the process. Figure 2 represents the TDCS of (e, 2e) for the outer valence shell of Ar ($3p$) where the projectile is scattered with an energy $E_a = 500$ eV and an angle $\theta_a = 6°$ while the ejected electron is detected with energies $E_b = 37$ and 74 eV [45]. As the measured cross sections are given on a relative scale they are normalized to the BBKSR model. It is noticeable that the two models reproduce quite well the binary region where the shape of the TDCS is correctly reproduced and the peak is well located. The theoretical description of the recoil region is on the other hand less good. BBK fails completely to reproduce the recoil peak which is clearly underestimated. When we introduce the short range potential via the BBKSR model, the results are somewhat improved. The recoil peak is well visibly enhanced, nevertheless the position of this peak is not correctly described. We should notice that both BBK and BBKSR models do not include distortion effects in the mechanism. A model like BBKDW with a contribution of the short range potential might describe better this experimental situation. Overall the short range potential seems to play a significant role in the recoil region.

The molecular targets CH_4, NH_3 and H_2O are at present investigated under different kinematical situations which would provide accurate information about the ionization dynamics. It is worth noting that these molecules have the same number of electrons but with different number of nuclei, their molecular orbitals are furthermore described by different symmetry groups.

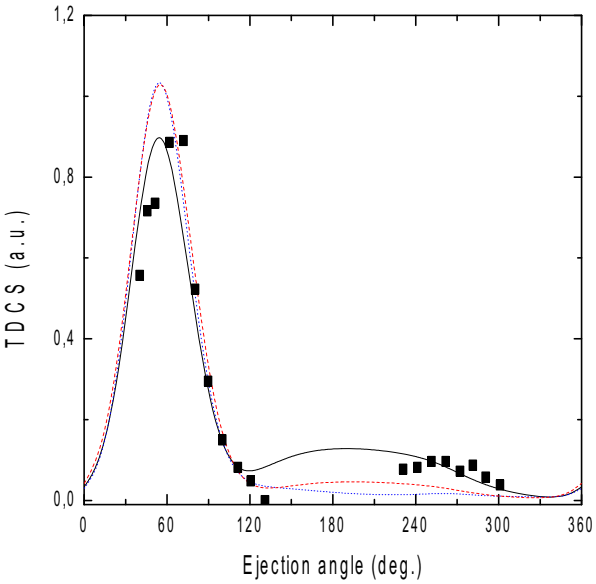

Fig. 3. Triple differential cross section for the ionization of CH_4 molecule in its ground state. The projectile with an energy $E_0 = 250$ eV is scattered at an angle $\theta_a = 10°$ in coincidence with the ejected electron with an energy $E_b = 50$ eV. Comparison is made between the experimental data (solid squares) of Isik et al. [41] and the theoretical models: (i) the BBKSR model (black solid line); (ii) the BBK model (red dashed line); (iii) the BBKDW model (blue dotted line). The experiments are normalized to the absolute scale of BBKSR for the best visual fit at the maximum of the binary region.

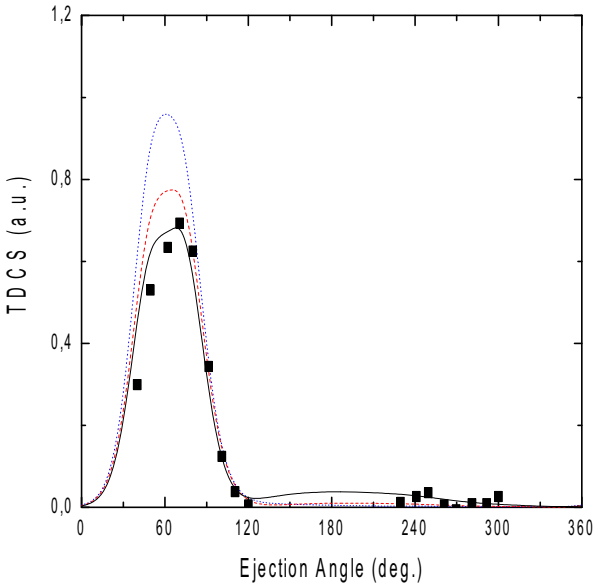

Fig. 4. Same as Figure 3 but for $\theta_a = 20°$.

The TDCS for 250 eV electron impact ionization of the $1t_2$ orbital of CH_4 very recently performed by Isik et al. [41] is presented in Figures 3 and 4 for two fixed scattering angles 10° and 20°, with 50 eV ejected electron energy. Our results within BBK, BBKDW and BBKSR models are displayed in their absolute scale while the data are normalized to BBKSR. We remind that the rather sophisticated model BBKDW failed very recently [33] to describe the recoil region for these two situations. We can see, for a scattered angle $\theta_a = 10°$ (corresponding to a momentum transfer of 0.9 au), that the binary peaks of the three models point in the same direction. The lobes of BBK and BBKDW in this region are of comparable intensities and overestimates somewhat the peak of BBKSR. Overall the shape of the TDCS in this region is qualitatively well reproduced by the three models. Nevertheless BBK and BBKDW models are not able to describe the recoil region contrary to BBKSR which clearly reproduces a recoil peak and exhibits the best agreement with experiments. Figure 4 represents the TDCS in the same conditions of Figure 3 but for a scattered angle $\theta_a = 20°$ corresponding to a momentum transfer of 1.5 au. We observe that the binary region is qualitatively well reproduced by the three models and the positions of the binary peaks point in the same direction. The amplitudes of the three models are quite different in this region, it is still observed that BBK and BBKDW binary amplitudes overestimate BBKSR one. The experimental recoil peak is better described by BBKSR while the two other models fail once again to exhibit any agreement with experiments in this region. We should indicate that the experimental data for these particular kinematics seem to be very sensitive to the momentum transfer, absolute measurements should provide more accurate information. As a preliminary conclusion, the BBKDW seems to play no role in recoil region, in the following discussion will focus only on BBK and BBKSR models.

We consider now the experiments of Orsay group for the same molecule [43] where both the outermost valence $1t_2$ and inner valence $2a_1$ orbitals are investigated. The measurements are performed at scattered electron energy of 500 eV, ejected electron energy of 74 eV and for scattering angle of 6°. The TDCS for the two orbitals is displayed in Figure 5 where all results are normalized to BBKSR since the data are relative, we also indicate that only BBK and BBKSR theoretical results are presented here. It is directly shown that the experimental data exhibit a large recoil scattering especially for the inner valence orbital $2a_1$. This is justified by the rather important value of the recoil momentum in this case ($q \approx 2$ au) which indicates that the residual ion actively participates to the process. The comparison between experiments and theory is rather satisfactory in the binary region, the two theoretical models give similar results and describe in the same way the process. On the other hand, the agreement is less good in the recoil region. The BBK model is not able at all to describe the process although the PCI is accounted while BBKSR shows a better agreement in this region. Indeed a more important recoil peak is shown for the two orbitals which means that the short range potential contributes significantly in this region. Unfortunately the experiments in the recoil region remain still poorly reproduced which indicates the need of more sophisticated treatments.

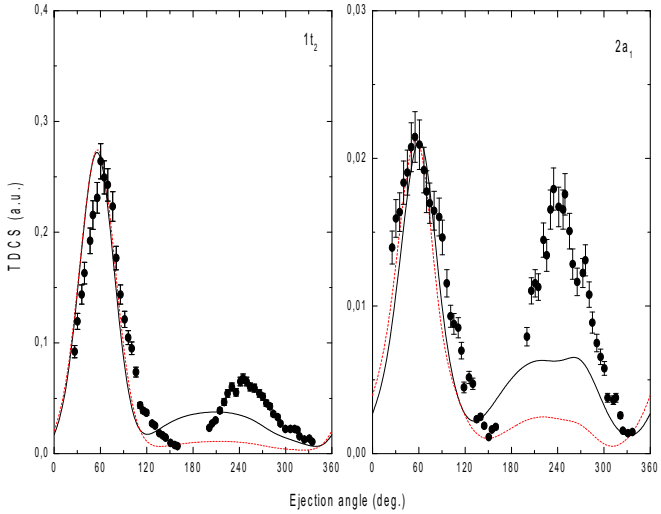

Fig. 5. Triple differential cross section for the ionization of $1t_2$ and $2a_1$ valence orbitals of CH_4 molecule in its ground state. The scattered electron with an energy $E_a = 500$ eV is detected at an angle $\theta_a = 6°$ in coincidence with the ejected electron with an energy $E_b = 74$ eV. Comparison is made between the experimental data [43] and the theoretical models: (i) the BBKSR model (black solid line); (ii) the BBK model (red dashed line. The experiments are normalized to the absolute scale of BBKSR for the best visual fit at the maximum of the binary region.

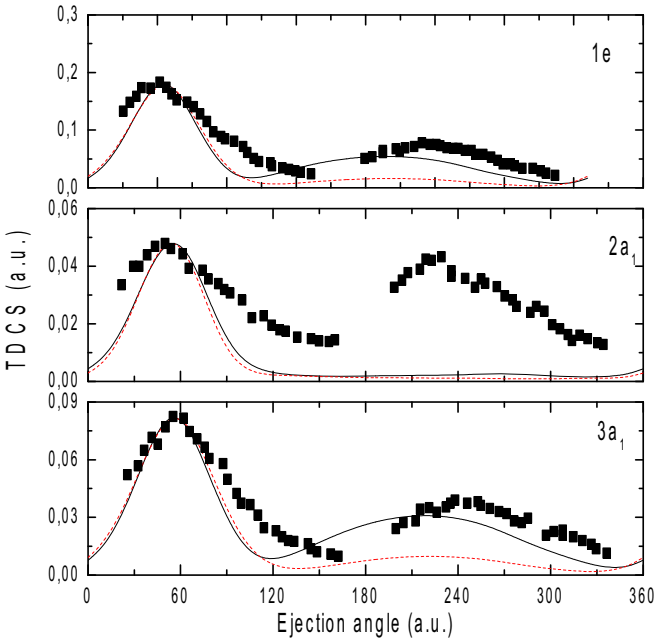

Fig. 6. Triple differential cross section for the ionization of $1e$, $2a_1$ and $3a_1$ valence orbitals of NH_3 molecule. The scattered electron with an energy $E_a = 500$ eV is detected at an angle $\theta_a = 6°$ in coincidence with the ejected electron with an energy $E_b = 74$ eV. Comparison is made between the experimental data [42] and the theoretical models: (i) the BBKSR model (black solid line); (ii) the BBK model (red dashed line). The experiments are normalized to the absolute scale of BBKSR for the best visual fit at the maximum of the binary region.

We consider now the ionization of NH_3 whose (e, 2e) process is investigated in the same conditions than for CH_4. Figure 6 presents a comparative study between our BBK and BBKSR theoretical models with the experiments performed at 500 eV scattered electron energy and 74 eV ejected electron energy [42]. The theoretical results are displayed in their absolute scale while the data are normalized to the BBKSR model at the binary peak as done for CH_4. It is seen that overall the two theoretical models exhibit nearly the same behavior in the binary region and agree quite well with experiments. We nevertheless notice that the width of the binary lobe is not correctly reproduced here, any other theory has in fact correctly reproduced the width of the binary lobe so far. The recoil region exhibits also an important lobe which is not reproduced by BBK for the three orbitals: $1e$, $2a_1$ and $3a_1$, as it has been already indicated in our former works [42,43]. In contrast, BBKSR model shows a better agreement in the recoil region where now the recoil peak is fairly well reproduced for the outer valence shells $1e$ and $3a_1$, showing once more the importance of the short range potential in the recoil region. It would mostly be mentioned that the positions of the experimental peaks are shifted towards higher angles with respect to the direction of the momentum transfer in the case of the two molecules (CH_4 and NH_3) which means contribution of non first order effects, this has been indeed predicted by the three models since they include systematically the PCI in the final state.

We finally study the TDCS of H_2O where experiments have been performed at 250 eV impact energy and a scattering angle of 15° with the ejected electron detected with an energy of 10 eV [46]. The investigation of this target has previously revealed that BBK model was able to describe correctly both the binary and the recoil regions [38] (except for the inner orbital $2a_1$). This was attributed later to the fact that the collision regime is quite close to Bethe-ridge conditions where the momentum transfer is fully absorbed by the ejected electron ($K = k_b$). It means that the effect of the target ion on the ejected electron is not strong. Conversely the kinematics used for CH_4 and NH_3 are far from the Bethe-ridge regime because the values of K and k_b are very different from each other. Since the outer shells have been shown to be rather well described by BBK and even by the first order model 1 CW [38], we investigate here only the inner valence orbital $2a_1$ of H_2O by applying BBK and BBKSR models. It is noticeable in Figure 7 that BBK fails completely to describe the recoil lobe as it was previously indicated. This allows to conclude that for this inner orbitals, in addition to PCI, other effects should be taken into account. When we apply BBKSR the behavior of the TDCS is substantially the same in the binary region when compared to BBK. However the recoil peak is slightly enhanced and seems to better describe the experiments but remains rather insufficient to explain the experiment. We could conclude anyway that the contribution of the short range potential plays a substantial role

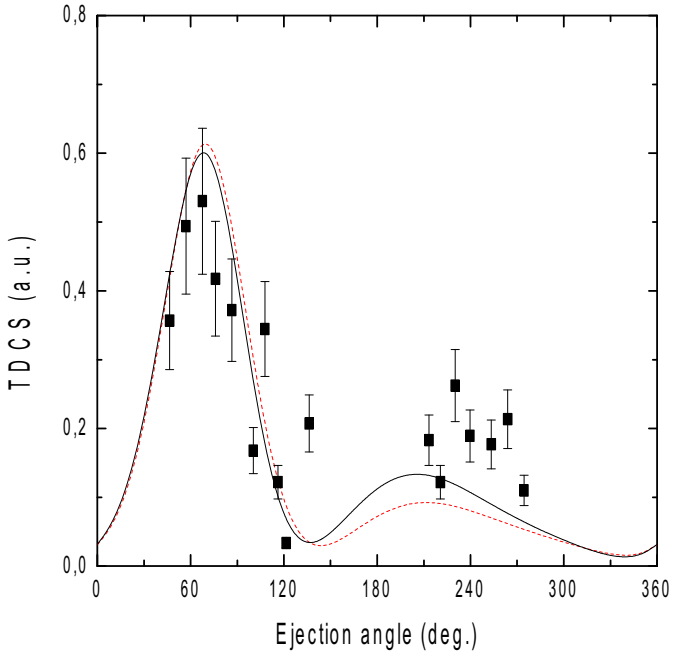

Fig. 7. Triple differential cross section for the ionization of the $2a_1$ inner valence orbital of H_2O molecule. The projectile with an energy $E_0 = 250$ eV is scattered at an angle $\theta_a = 15°$ in coincidence with the ejected electron with an energy $E_b = 10$ eV. Comparison is made between the experimental data [46] and the theoretical models: (i) the BBKSR model (black solid line); (ii) the BBK model (red dashed line). The experiments are normalized to the absolute scale of BBKSR for the best visual fit at the maximum of the binary region.

in the recoil region as was overall the case of the other targets studied above.

4 Conclusion

In the present paper, we have performed calculations to study the (e, 2e) collision for atomic and molecular targets using models which include the electron-electron interaction in the final state to all orders of perturbation theory. Three theoretical models (BBK, BBKDW BBKSR) have been used in this context to study argon atom and some specific molecules (H_2O, CH_4 and NH_3). It has been observed that the three models are able to well describe the positions of the binary and recoil peaks which are shifted with respect to the momentum transfer direction at low impact energies. This was expected since these models represent non first order approaches. The three models describe qualitatively in the same way the binary region. BBKDW reproduces better the binary region when absolute measurements are present but fails completely to describe the recoil peak region like the BBK model. When BBKSR is applied the recoil region is better reproduced but it remains insufficient in some cases to predict the data. The short range potential, which is usually omitted, seems to play an important role in the recoil region. A merger of BBKDW with BBKSR should improve the theoretical results bearing in mind that this method requires very powerful computation means. Work in this aspect is currently in progress.

Author contribution statement

All authors contributed equally to the paper.

References

1. C. Stia, O. Fojon, P. Weck, J. Hanssen, B. Joulakian, R.D. Rivarola, Phys. Rev. A **66**, 052709 (2002)
2. C. Champion, J. Hanssen, P.A. Hervieux, J. Chem. Phys. **117**, 197 (2002)
3. M. Inokuti, Rev. Mod. Phys. **43**, 297 (1971)
4. J. Colgan, M.S. Pindzola, Phys. Rev. A **74**, 012713 (2006)
5. C. Dal Cappello, Z. Rezkallah, S. Houamer, I. Charpentier, P.A. Hervieux, M.F. Ruiz-Lopez, R. Dey, A.C. Roy, Phys. Rev. A **84**, 032711 (2011)
6. A.O. Bawagan, R. Müller-Fiedler, C.E. Brion, E.R. Davidson, C. Boyle, Chem. Phys. **120**, 335 (1988)
7. B.P. Hollebone, Y. Zheng, C.E. Brion, E.R. Davidson, D. Feller, Chem. Phys. **171**, 303 (1993)
8. P.L. Bartlett, A.T. Stelbovics, Phys. Rev. A **66**, 012707 (2002)
9. J.P. Santos, F. Parente, Eur. Phys. J. D **47**, 339 (2008)
10. J. Colgan, M.S. Pindzola, G. Childers, M.A. Khakoo, Phys. Rev. A **73**, 042710 (2008)
11. S. Houamer, A. Mansouri, C. Dal Cappello, A. Lahmam-Bennani, S. Elazzouzi, M. Moulay, I. Charpentier, J. Phys. B **36**, 3009 (2003)
12. I. Tóth, R.I. Campeanu, L. Nagy, Eur. Phys. J. D **69**, 2 (2015)
13. M. Cherid, A. Lahmam-Bennani, A. Duguet, R.R. Zurales, R.W. Lucchese, M.C. Dal Cappello, C. Dal Cappello, J. Phys. B **22**, 3483 (1989)
14. D.H. Madison, K. Bartschat, J.L. Peacher, Phys. Rev. A **44**, 304 (1991)
15. A. Kheifets, J. Phys. B **26**, 2053 (1993)
16. A. Kheifets, I.E. McCarthy, D.H. Madison, E. Weigold, J. Phys. B **31**, 2187 (1998)
17. D.H. Madison, Phys. Rev. Lett. **53**, 42 (1984)
18. I. Bray, J. Phys. B **33**, 581 (2000)
19. I. Bray, D.V. Fursa, A.S. Kheifets, A.T. Stelbovics, J. Phys. B **35**, R117 (2002)
20. K. Bartschat, O. Vorov, Phys. Rev. A **72**, 022728 (2005)
21. O. Zatsarinny, K. Bartschat, Phys. Rev. A **85**, 062709 (2012)
22. M. Brauner, J.S. Briggs, H. Klar, J. Phys. B **22**, 2265 (1989)
23. A. Mansouri, C. Dal Cappello, S. Houamer, I. Charpentier, A. Lahmam-Bennani, J. Phys. B **37**, 1203 (2004)
24. C. Dal Cappello, I. Charpentier, S. Houamer, P.A. Hervieux, M.F. Ruiz-Lopez, A. Mansouri, A.C. Roy, J. Phys. B **45**, 175205 (2012)
25. A. Prideaux, D.H. Madison, Phys. Rev. A **67**, 052710 (2003)
26. S. Jones, D.H. Madison, A. Franz, P.L. Altick, Phys. Rev. A **48**, R22 (1993)

27. J. Gao, D.H. Madison, J.L. Peacher, J. Chem. Phys. **123**, 304314 (2005)
28. H. Chaluvadi, C.G. Ning, D.H. Madison, Phys. Rev. A **89**, 062712 (2014)
29. F. Catoire, E.M. Staicu Casagrande, M. Nekkab, C. Dal Cappello, K. Bartschat, A. Lahmam-Bennani, J. Phys. B **39**, 2827 (2006)
30. X. Ren, T. Pflüger, J. Ullrich, O. Zatsarinny, K. Bartschat, D.H. Madison, A. Dorn, Phys. Rev. A **85**, 032702 (2012)
31. C.J. Colyer, S.M. Bellm, B. Lohmann, G.F. Hanne, O. Al-Hagan, D.H. Madison, C.G. Ning, J. Chem. Phys. **133**, 124302 (2010)
32. V.V. Serov, V.L. Derbov, B.B. Joulakian, S.I. Vinitsky, Phys. Rev. A **75**, 012715 (2007)
33. M. Chinoune, S. Houamer, C. Dal Cappello, A. Galstyan, J. Phys. B **49**, 205201 (2016)
34. E. Clementi, C. Roetti, A. Data Nucl. Data Tables **14**, 177 (1974)
35. R. Moccia, J. Chem. Phys. **40**, 2164 (1964)
36. R. Moccia, J. Chem. Phys. **40**, 2176 (1964)
37. R. Moccia, J. Chem. Phys. **40**, 2186 (1964)
38. C. Champion, C. Dal Cappello, S. Houamer, A. Mansouri, Phys. Rev. A **73**, 012717 (2006)
39. C. Dal Cappello, Z. Rezkallah, S. Houamer, I. Charpentier, A.C. Roy, P.A. Hervieux, M.F. Ruiz-Lopez, Eur. Phys. J. D **67**, 117 (2013)
40. M.A. Kornberg, J.E. Miraglia, Phys. Rev. A **48**, 3714 (1989)
41. N. Isik, M. Dogan, S. Bahceli, J. Phys. B **49**, 065203 (2016)
42. R. El Mir, E.M. Staicu Casagrande, A. Naja, C. Dal Cappello, S. Houamer, F. El Omar, J. Phys. B **48**, 175202 (2015)
43. A. Lahmam-Bennani, A. Naja, E.M. Staicu Casagrande, N. Okumus, C. Dal Cappello, I. Charpentier, S. Houamer, J. Phys. B **42**, 165201 (2009)
44. A. Lahmam-Bennani, H.F. Wellenstein, A. Duguet, A. Daoud, Phys. Rev. A **30**, 1511 (1984)
45. A. Kheifets, A. Naja, E.M. Staicu Casagrande, A. Lahmam Bennani, J. Phys. B **41**, 145201 (2008)
46. D.S. Milne-Brownlie, S. Cavanagh, B. Lohmann, C. Champion, P.A. Hervieux, J. Hanssen, Phys. Rev. A **69**, 032701 (2004)